Estuarine, Coastal and Shelf Science 259 (2021) 107432

Contents lists available at ScienceDirect

Estuarine, Coastal and Shelf Science

journal homepage: www.elsevier.com/locate/ecss

Mangrove carbon stocks in Pongara National Park, Gabon

Carl C. Trettin [a,*], Zhaohua Dai [a,b], Wenwu Tang [c], David Lagomasino [d], Nathan Thomas [e], Seung Kuk Lee [f], Marc Simard [g], Médard Obiang Ebanega [h], Atticus Stoval [i], Temilola E. Fatoyinbo [i]

[a] USDA Forest Service, Southern Research Station, Cordesville, SC, USA
[b] School of Forest Resources and Environmental Science, Michigan Technological University, Houghton, MI, USA
[c] Center for Applied GIScience, University of North Carolina – Charlotte, Charlotte, NC, USA
[d] Dept. Coastal Studies, East Carolina University, Greenville, NC, USA
[e] University of Maryland, Greenbelt, MD, USA
[f] Dept. of Earth and Environmental Sciences, Pukyong National University, Busan, Republic of Korea
[g] National Aeronautics and Space Administration, Jet Propulsion Laboratory, Pasadena, CA, USA
[h] Omar Bongo University, Libreville, Gabon
[i] National Aeronautics and Space Administration, Goddard Space Flight Center, Greenbelt, MD, USA

ARTICLE INFO

Keywords:
Rhizophora
Blue carbon
Forested wetland
Mangrove inventory

ABSTRACT

Mangroves are recognized for their valued ecosystem services to coastal areas, and the functional linkages between those services and ecosystem carbon stocks have been established. However, spatially explicit inventories are necessary to facilitate management and protection of mangroves, as well as providing a foundation for payment for ecosystem service programs such as REDD+. We conducted an inventory of carbon stocks in mangroves within Pongara National Park (PNP), Gabon using a stratified random sampling design based on forest canopy height derived from TanDEM-X remote sensing data. Ecosystem carbon pools, including aboveground and belowground biomass and necromass, and soil carbon to a depth of 2 m were assessed using measurements and samples from plots distributed among three canopy height classes within the park. There were two mangrove species within the inventory area in PNP, *Rhizophora racemosa* and *R. harrisonii*. *R. harrisonii* was predominant in the sparse, low-stature stands that dominated the west side of the park. In the east side of the park, both species occurred in tall-stature stands, with tree height often exceeding 30 m. Canopy height was an effective means to stratify the inventory area, as biomass was significantly different among the height classes. Despite those differences in aboveground biomass, the soil carbon density was not significantly different among height classes. Soils were the main component of the ecosystem carbon stock, accounting for over 84% of the total. The ecosystem carbon density ranged from 644 to 943 Mg C ha^{-1} among the three height classes. The ecosystem carbon stock within PNP is estimated to be 40,588 Gg C. The combination of pre-inventory information about stand conditions and their spatial distribution within the assessment area obtained from remote sensing data and a spatial decision support system were fundamental to implementing this relatively large-scale field inventory. This work exemplifies how mangrove carbon stocks can be quantified to augment national C reporting statistics, provide a baseline for projects involving monitoring, reporting and verification (i.e., MRV), and provide data on the forest composition and structure for sustainable management and conservation practices.

1. Introduction

Mangrove ecosystems provide many valuable goods and services to coastal areas, including shoreline stabilization, aquatic habitat and fisheries, forest products and food. Mangroves are also recognized for their role in the global carbon (C) cycle (Alongi, 2012). Mangroves are among the most carbon-rich forest types in the tropics (Donato et al., 2011), and sediments are the largest C pool, contributing much more than biomass to the ecosystem C stock (Kauffman et al., 2011; Attwood et al., 2017; Hamilton and Friess, 2018). The provision of ecosystem

* Corresponding author. 3734 Hwy 402, Cordesville, SC, 29434, USA.
E-mail address: carl.c.trettin@usda.gov (C.C. Trettin).

https://doi.org/10.1016/j.ecss.2021.107432
Received 8 April 2020; Received in revised form 3 May 2021; Accepted 20 May 2021
Available online 31 May 2021

services from mangroves is inextricably linked to the integrity of the ecosystem C pools (Alongi, 2011).

Deforestation and forest degradation constitute the second largest anthropogenic source of carbon dioxide to the atmosphere, after fossil fuel combustion, comprising 8–20% of anthropogenic emissions (van der Werf et al., 2009; IPCC, 2019). The loss of mangroves is an important contributor to those emissions with approximately 38% of the global mangrove resource experiencing degradation (Thomas et al., 2017); fortunately the rate of deforestation is declining globally (Hamilton and Casey, 2016). While the reduction in mangrove area is primarily attributed to anthropogenic activities (Ong, 1995; Friess et al., 2020), natural factors such as erosion and storm degradation also cause losses (Thomas et al., 2017). Mangroves are dynamic ecosystems and not all change is negative. For example, mangrove forests in deltaic systems may exhibit a net increase in area due to sediment deposition (Shapiro et al., 2015), and mangrove area may also increase in response to climate change (Friess et al., 2020). This dynamic nature of mangroves infuses uncertainty in assessments of large-scale change analyses of mangrove area (Friess and Webb, 2014). Accordingly, critical factors for assessing the C stocks in mangroves under any MRV (Monitoring, Reporting and Verification) protocol are (a) quantification of the C stocks, and (b) assessment of the change in stocks over time.

The loss of C from disturbance regimes in mangroves is currently estimated to be between 20 and 450 MT CO_2e yr^{-1}, which is a disproportionately high rate given the relatively small area of mangroves globally compared to other forest types (Friess et al., 2020). Land use change is the principal cause of the C emissions from mangroves (Friess et al., 2020; Hamilton and Friess, 2018), which is the motivation for reducing emissions through conservation, sustainable management, and the inclusion of mangroves in payment for ecosystem services programs, such as Reducing Emissions from Deforestation and Forest Degradation (REDD+).

In order to manage and protect mangroves or to commoditize mangrove carbon stocks, spatially explicit inventories are required (Locatelli et al., 2014). Correspondingly, an objective assessment based on randomly located plots is necessary to estimate the forest composition, structure and the associated carbon stocks. One of the challenges in conducting inventories in many mangroves forests is the lack of baseline or background information. Forest canopy height derived from remote sensing data is functionally related to stand biomass (Fatoyinbo and Simard, 2013; Feliciano et al., 2017); hence it's a logical data platform for designing an inventory of mangroves (Stringer et al., 2015). Other attributes, such as geomorphic position, could also be used in the inventory design.

Gabon accounts for approximately 1% of global mangrove area, and approximately 5.6% of total mangrove area in Africa (Giri et al., 2011; Fatoyinbo and Simard, 2013). Within Gabon, approximately 43% of the mangroves occur in the Gabon Estuary, based on the Giri et al. (2011) distribution of mangroves. Gabon is known to contain tall-stature mangroves, and Pongara National Park (PNP) on the south bank of the Gabon Estuary is the site of the world's tallest mangrove (Simard et al., 2019). The mean loss of mangroves to land use change in Gabon have been reported to range from 0.5% yr^{-1} for the period 2000–2014 (Hamilton and Casey (2016) to 2.7% between 2000 and 2010 (Ajonina et al., 2014a), rates higher than the global average (0.13% yr^{-1}) during the period 2000–2016 (Goldberg et al., 2020).

In this study, we quantified mangrove carbon stocks in PNP which contains approximately 37% of the mangroves in Gabon. We accomplished this goal by (1) using high-resolution TanDEM-X remote sensing data to stratify mangroves into spatially explicit canopy height classes, (2) quantifying and comparing carbon stocks across canopy height classes within a section of the park, and (3) using mangrove extent and canopy height classes in the park to scale-up ecosystem C stocks to the landscape-level. This was done to further the development of methodologies for objectively inventorying mangroves that could be used for REDD + project assessments, MRV, and active management and conservation of mangroves. This work builds on another large-scale assessment of C stocks in the Zambezi River Delta (Stringer et al., 2015) where we used remote sensing data to enhance field-based inventories to quantify mangrove carbon stocks. Our goal is to demonstrate the applicability of this approach on two common landforms that contain mangroves: estuaries and deltas. We selected Gabon for the study because the U.S. National Aeronautics and Space Administration (NASA) has developed both aircraft and satellite based remote sensing data that included the Gabon Estuary, thereby providing data and opportunity to compare different data products and their applicability of mangrove assessments. PNP was also known to have a wide range in mangrove stand conditions, canopy height ranging from 2 to >63 m (Lee et al., 2018; Simard et al., 2019). This work also complements the recently completed national soil C inventory conducted in Gabon (Wade et al., 2019) by illustrating how an ecosystem that is under represented in the national inventory (e.g., mangroves) can be considered through quantification of C stocks in a resource-specific inventory.

2. Methods

2.1. Study area

Pongara National Park contains internationally recognized wetlands of importance through the Ramsar Convention; it's located on the south bank of the Gabon Estuary (Fig. 1), within 0.013° S – 0.35° N and 9.3°–9.96° E, comprising approximately 96,302 ha (Ramsar Sites Information Service, 2015). The estuary receives water from the Komo and Ebe Rivers, and drains westerly into the Gulf of Guinea, Atlantic Ocean. The estuary is characterized as relatively short and wide, with mangroves occurring along the north and south banks. Pongara National Park encompasses the expansive south bank of the Gabon Estuary, containing approximately 53,379 ha of mangroves (Giri et al., 2011) which is approximately 55% of the total area of the park.

Gabon has a tropical climate, with two distinct seasons, rainy (September–May) and dry (June–August). The annual precipitation ranges from 2400 mm on the eastern, upstream side of the estuary to 2830 mm on western side at the estuary mouth to the Atlantic Ocean (Hijmans et al. 2005). The rainy period has two peak periods (October and May). The range in annual mean temperature within PNP is small, averaging approximately 26.3 ± 0.9 °C. The mean monthly maximum and minimum temperatures are 29.7 ± 1.2 °C and 22.9 ± 0.7 °C respectively (Hijmans et al. 2005).

2.2. Inventory design

We used a stratified random sampling design for the inventory, as an inventory of the mangroves in the Zambezi River delta demonstrated that to be an effective design (Stringer et al., 2015). Forest canopy height, derived from high resolution TanDEM-X remote sensing data (Lee et al., 2018) was used as the basis for stratification. The application of this sampling design is based on the ability to estimate mangrove canopy height from remote sensing data (Simard et al. 2006; Lagomasino et al., 2016), the understanding of relationships between mangrove canopy height and biomass using Tan DEM-X data (Feliciano et al., 2017), and our experience of using canopy height as the basis for an objective inventory of mangroves and estimation of carbon stocks (Stringer et al., 2015). Based on the distribution of remotely sensed canopy height , pixels containing mangroves were delineated using the mangrove coverage developed by Giri et al. (2011). Three canopy height classes were identified: HTC1 (1–11 m), HTC2 (11–21 m) and HTC3 (≥21 m); these classes were selected to allocate approximately equal areas within each class. As a result, HTC3 had the widest range in height with the maximum tree height exceeding 50 m.

Given the large size of PNP and practical constraints on the number of field plots that was feasible to measure, two blocks within the park were selected that represented the mosaic of stand conditions, as

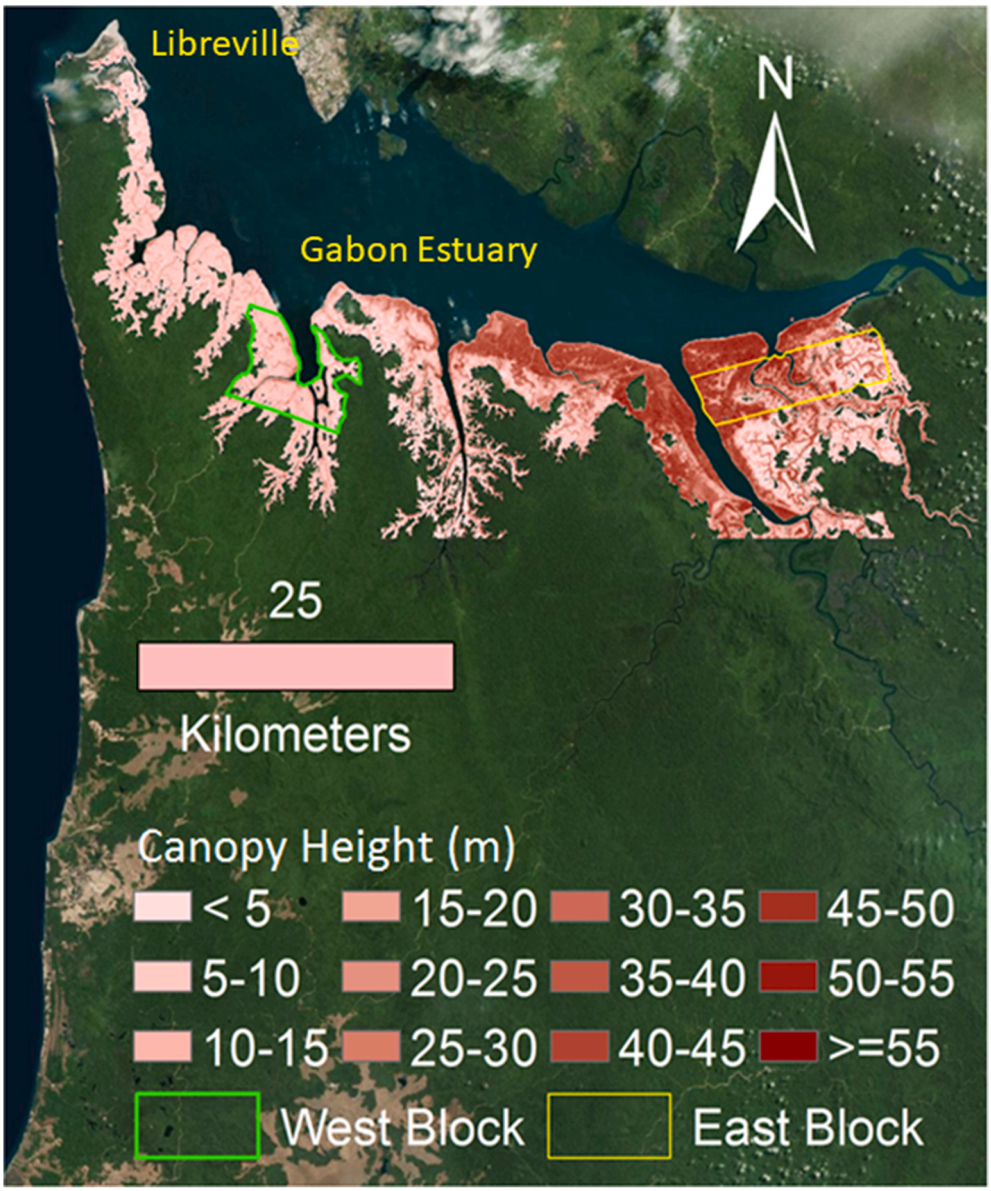

Fig. 1. Distribution of mangroves within Pongara National Park and forest canopy height (m) based on TanDEM-X data (Lee et al., 2018). The east and west inventory blocks are shown as insets. (Image by: W. Feng, Univ. North Carolina - Charlotte).

inferred from canopy height (Fig. 1). The east block contained a larger proportion of HTC3 stands, while the west block contained a larger proportion of low stature HTC1 stands; however, each height class was represented within the two blocks. The combined area of the inventory blocks was 9,200 ha or approximately 17% of the mangrove area in PNP. Seventeen plots were used, distributed by HTC1: 4 plots, HTC2: 4 plots, and HTC3: 9 plots.

A spatial decision support system (SDSS) was used to ensure that the plots were randomized within the height class strata (Tang et al., 2016). Potential areas for locating an inventory plot were 0.5 ha in size to ensure relatively uniform conditions within the sampling area. The SDSS also provided capacity to address logistical constraints, such as camp location, the distance from camp (e.g. transit time), and accessibility (e.g., hiking/climbing distance). Each plot had randomly selected alternates pre-selected, in case the selected plot was not able to be used because of unanticipated difficulties. The inventory plot was circular (0.04 ha); if trees greater than 50 cm DBH were observed, the plot area was increased to 0.05 ha, and for low stature, sparse stands (e.g., height < 4 m), the area was reduced to 0.01 ha.

The carbon pools considered in this inventory are the above- and below-ground biomass, and soils because these comprise the majority (e.g., >98%) of the ecosystem carbon. Ground vegetation and down-dead wood typically comprises less than 2% of the mangrove biomass (Kauffman and Donato, 2012). Field work was conducted in February 2017.

2.3. Tree biomass

Diameter at breast height (DBH), total tree height, which was measured with a Haglöf Vertex III® hypsometer, and species were recorded for all live trees within the inventory plot. Overstory trees, (DBH $\geq$ 5 cm) were measured within the entire plot, while trees (DBH$<$ 5 cm) were measured within a 2 m diameter subplot located around plot center. Aboveground and belowground biomass were estimated for each tree using published allometric equations developed by Ajonina (2008) for Central Africa, which use DBH and wood density as the input parameters (Eqn. (1) and (2)).

$$AGB_i = \rho \times V_i \quad (1)$$

$$BGB_i = \alpha \times V_i \quad (2)$$

where $AGB_i$and $BGB_i$are aboveground biomass (AGB) and belowground biomass (BGB) of ith individual tree, respectively; V_i is the corresponding tree volume (see Eqn, 3, 4); ρ is wood density. We used ρ = 1.02 g cm^{-3} for both *Rhizophora* species which is the median value for *Rhizophora* in Africa (Carson et al. 2012) with a reported range of 0.91–1.14 g cm^{-3}. The coefficient used to estimate mangrove root biomass in Eqn. (2) is:

$$\alpha = 1.385 \times DBH^{-0.4331} \quad (3)$$

where DBH (cm) range: 1 ≤ DBH≤102.8 cm (Ajonina et al., 2014b). The volume (V) was estimated as:

$$V = 0.0000733 \times DBH^{2.7921} \quad (4)$$

where V is in cubic meter (m^3), DBH in cm. The biomass (kg) of each tree was summed and divided by the plot area (hectare) to estimate biomass density per unit area (Mg ha^{-1}). Biomass estimates were converted to C using the published C concentration of 0.50 and 0.39 for above-ground and below-ground biomass, respectively (Kauffman and Donato, 2012).

2.4. Standing tree necromass

Above- and below-ground necromass for standing dead trees was determined in different ways depending on decay class (Kauffman and Donato, 2012). For the above-ground necromass decay classes 1 and 2, the allometric equation for live trees was applied, using a density (ρ) of 0.69 g cm^{-3}; a reasonable estimate of large solid dead wood (Kauffman and Donato, 2012). The above-ground necromass for decay class 3 standing dead trees was determined by applying the formula of the volume of a cone (Eqn. (5)) multiplied by the wood density (Eqn. (6)):

$$\boldsymbol{V = \pi r^2 \frac{h}{3}} \quad (5)$$

$$AGB - D_3 = V^* \rho \quad (6)$$

where: V is volume (m^3), r is $\frac{DBH}{2}$ (m), h is the tree height (m), and ρ is wood density (0.69 g cm^{-3}), and AGB-D_3 is necromass (kg). Similar to live trees, the necromass of dead trees was integrated into necromass density (Mg ha^{-1}), and necromass carbon density using the same conversion factors used for live trees.

2.5. Soil

The soil was sampled to a depth of 200 cm from 3 random points within the inventory plot using a 1 m gouge auger (AMS Inc., American Falls, Idaho, USA). For each soil core, volumetric subsamples, typically 5–8 cm in length, were extracted from the center of 6 pre-determined soil strata beneath the surface (0–15, 15–30, 30–45, 45–110, 110–180, 180–200 cm). Subsamples from the same soil strata across cores were subsequently combined into one composite soil sample per stratum. Samples were placed in pre-labeled sealed containers. Samples were stored at ambient temperature during the field mission and transit to the laboratory. Upon receipt at the laboratory, soil samples were dried at 105 °C until a constant weight was achieved; the dry sample mass was subsequently measured. The soil bulk density (g cm^{-3}) of each sample was calculated by dividing the oven-dried mass by the sample volume. To provide a general characterization of soil pH, samples of each strata from eight plots (HTC1: 2, HTC2: 3, HTC3: 3) were measured using a 4:1 ratio of deionized water and soil (Thomas, 1996).

The soil organic C (SOC) concentration of each soil sample was determined at the Center for Applied Isotope Analyses, University of Georgia, USA. Pulverized subsamples were analyzed using a Carlo Erba, NA1500 CHN Analyzer (Carlo Erba Strumentazione, Milan, Italy) via a Thermo Conflo III open split interface. Quality assurance was provided by the analysis of duplicates (every 10th sample), blind standards (certified standard, every 20th sample) and calibration of the instrument with certified standards. The precision of duplicate samples was <± 0.1% for C.

Particle size distribution of soils from eight plots representing the three HTC (HTC1: 2, HTC2: 3, HTC3: 3) was analyzed by laser diffraction using a Malvern Mastersizer 2000 at the Environmental Soil Analysis Laboratory, Univ. Nevada – Las Vegas. The following particle sizes classes are reported for the sampled soil layers: clay (<2 μm), silt (2–50 μm), fine silt (2–20 μm), and sand (0.05–2 mm).

Soil C density within each sampling strata was determined as follows:

$$\boldsymbol{C_S^n = D_b \times l \times C \times 100} \quad (7)$$

where: C_S^n is the SOC concentration (Mg C ha^{-1} for SOC) for strata n (n = 1, 2, …,6), D_b is the bulk density (g cm^{-3}), l is the strata interval length (cm), and C is the sample C concentration, expressed as a fraction. The C density of each layer within a core was summed to determine the total soil C density to a depth of 200 cm for the plot.

Conductivity of the soil pore water was measured by sampling water collected by excavating a shallow surface hole approximately 15 cm deep and allowing it to refill for 2–3 h. Water was sampled from the hole using a 50 cc syringe, which was then tested for conductivity using a Myron L Ultrameter II 4PII (Myron L, Carlsbad, CA, USA). Prior to measurement, the sample cell was rinsed three times with collected water and then refilled for measurement. Conductivity was converted to salinity following Standard Methods for the Examination Water and Wastewater Analysis (Baird and Bridgewater, 2017).

2.6. Statistical analyses

Two-way analysis of variance was used to assess differences in measured and calculated variables. The two fixed factors were block (e.g., east, west) and canopy height class. Analyses were conducted using SigmaPlot (Systat Software Inc., Ver. 14, 2018); homogeneity of variance was assessed with the Brown-Forsythe test and significance differences were considered at $P < 0.05$. Soil chemical and physical properties were analyzed averaging within layers, thereby enabling an assessment of the depth distribution of the properties. The soil C content was calculated as the sum of the C content of each strata. Carbon stocks within the inventory blocks were estimated by utilizing the mean C density for AGB, BGB and soil for each canopy height class multiplied by the area. Ecosystem C (EC) is the sum of the total AGB, BGB, including biomass and necromass, and soil stocks. The total C stock for the mangroves within PNP was estimated by applying the EC density measured in the two inventory blocks to the three canopy height classes that had been delineated for mangroves within the park.

3. Results

3.1. Forest composition & structure

Although seven mangrove species are reported to occur in Gabon (FAO, 2007), only two (*Rhizophora harrisonii* and *R. racemosa),* occurred within the inventoried area in PNP. The stands tended to be monotypic with only one stand containing both species. Across the inventoried area, *R. harrisonii* accounted for 51.3% of the stems, while *R. racemosa* accounted for 48.7%. The species mix within height classes were similar for HTC 1 and 3, with *R. harrisonii* comprising 50 and 44% of the stems, respectively. In HTC 2, 75% of the stems were *R. harrisonii*. Distribution of species varied across the inventoried areas. The west block was dominated by *R. harrisonii*, accounting for 79.5% of the total number of stems, and *R. racemosa* only occurred as HTC3 stands. In contrast, the

east block was dominated by *R. racemosa*, and *R. harrisonii* was only found in the HTC3 stands.

Average tree diameter varied from 4.3 cm in HTC1 to 19.8 cm in HTC3, while the average tree height ranged from 2.8 m in HTC1 to 19.9 m in HTC3; however, only the mean diameter and height in HTC1 and HTC3 were significantly different (Table 1). The stands in the east inventory block tended to be taller than those in the west inventory block but they weren't significantly different (average tree height east block = 10.9 m, west block = 8.0 m, p = 0.57). The tallest tree measured during the inventory was 52.5 m, which it was sampled in the general vicinity of where Simard et al. (2019) reported the world's tallest mangrove (62.8 m). There was a strong linear relationship between the height of the tallest tree in the plot and the average tree height up to approximately 30 m; beyond that maximum tree height the relationship became erratic (Supplemental Fig. 1). Stocking in the mangrove stands declined with in an increase in canopy height, where the mean stocking of live trees was 4,280, 2861 and 724 trees ha^{-1} in HTC1, HTC2 and HTC3, respectively (Table 1). The stocking within canopy height classes was significantly different ($P < 0.01$) between the east and west inventory blocks. In the east block, the mean stocking was 1,322 trees ha^{-1}, and the stocking levels weren't significantly different among HTCs; while stocking averaged 6,454, 3,448, and 648 trees ha^{-1} in HTC1 to HTC3 respectively in the west inventory block, and they were significantly different ($P < 0.05$) from each other. Accordingly, overall the stands were significantly denser in the west block (mean 3517 trees ha^{-1}) than in the east inventory block. Despite the difference in stocking between the east and west inventory blocks, the average stand basal area was not statistically different (east block = 10.9, west block = 10.3 m^2 ha^{-1}; P = 0.89). However, the basal area in HTC1 was significantly less than stands in HTC3 (Table 1) across the inventoried areas within PNP.

The relationship of stand stocking and average stand diameter exhibited the J-shaped curve that is typical of uneven-aged forested landscapes (Fig. 2a). Stocking also exhibited the same relationship with average tree height (Fig. 2a). Average stand diameter and tree height exhibited a strong relationship ($P < 0.001$), that can be described by a sigmoidal function (Fig. 2b). Conversely, stand basal area was not as an effective predictor of average tree height (Supplemental Fig. 2), because mean tree height tended to maximize near 20 m across the range of observed stand densities, except for two very tall-stature stands (mean height > 35 m). There was also one stand in the inventory with a very high stand density (>45 m^2 ha^{-1}).

There were large differences in live tree biomass in the inventoried area reflecting the wide variation in stocking and tree diameter. Above-ground biomass on the HTC1 averaged 5.0 Mg ha^{-1} while the average for HTC3 was 375.7 Mg ha^{-1} (Table 1). Below-ground biomass varied similarly, ranging from an average of 4.1 Mg ha^{-1} in HTC1 to 106.0 Mg ha^{-1} in HTC3 (Table 1). Differences in biomass among the east and west inventory blocks weren't significant (P = 0.79). Necromass contributed by standing dead wood and the trees <5 cm DBH accounted for a small fraction of total biomass; approximately 0.72% of total AGB and 0.66% of total BGB was contributed by standing dead wood, and 0.5% of the total AGB and 1.6% of the total BGB contributed by the live understory trees (<5 cm DBH).

There is a strong correlation between stand biomass and basal area (Fig. 2c), which is a useful relationship for forest managers since basal area is a convenient metric obtainable in the field. A similarly strong relationship exists for below-ground biomass and total biomass (Supplemental Fig. 3). The correspondence between stand basal area and biomass is attributable to the fact that both are derived from tree DBH. Correspondingly and analogous to the relationship between average tree height and stand basal area, average above-ground biomass was invariant once the average tree height of the stand exceeded 15 m, unless the stand was exceedingly dense (Supplemental Fig. 4).

Table 1
Mean and standard error of tree diameter at breast height (DBH), tree height, stocking, basal area (BA), above-ground biomass (AGB) and below-ground (BGB) biomass for mangrove stands in the three canopy height classes (HTC).

Height Class	DBH (cm)	Height (m)	Stocking (trees ha^{-1})	BA (m^2 ha^{-1})	AGB (Mg ha^{-1})	BGB (Mg ha^{-1})
HTC1	4.3^{a}	2.8^{a}	4280^{a}	2.1^{a}	5.0^{a}	4.1^{a}
	(1.3)	(0.3)	(1412)	(0.2)	(0.7)	(0.4)
HTC2	$6.3^{a,b}$	$5.7^{a,b}$	$2861^{a,b}$	$7.1^{a,b}$	$38.8^{a,b}$	$20.3^{a,b}$
	(1.6)	(1.3)	(1112)	(2.3)	(15.7)	(7.3)
HTC3	19.8^{b}	19.9^{b}	724^{b} (163)	22.5^{b}	375.7^{b}	106.0^{b}
	(3.4)	(3.4)		(3.5)	(85.5)	(20.0)

Note: Different superscripted letters indicate significant difference ($p < 0.05$) within each of the stand structure metrics.

3.2. Soil properties

Soil bulk density (BD) increased with an increase in soil depth (Fig. 3a) from 0.24 g cm^{-3} in the 0–15 cm depth to 0.40 g cm^{-3} at 180–200 cm. There were no statistical differences in BD among the inventory blocks (P = 0.36) or canopy height classes (P = 0.31). The upper 50 cm of the soil is dominated by sand-size particles, below that depth silt predominates (Fig. 3b). The contrasting changes in the depth distribution of the sand and silt fractions are described well by exponential and power functions, respectively. Clay averaged less than 20% within the soil and increased with depth. Clay and silt in both blocks increased significantly ($R^2 = 0.91$, $P < 0.01$) with an increase in soil depth, and sand decreased ($R^2 = 0.91$, $P < 0.01$) with increasing soil depth soil depth (Fig. 3b). The difference in soil particle size classes among the two inventory blocks wasn't significant: sand (P = 0.06), silt (P = 0.07) and clay (P = 0.06).

Salinity of the soil pore water was significantly different ($P < 0.001$) among the two inventory blocks. The east block had an average salinity of 3.2 ppt while the west block averaged 21.5 ppt. The soil pore water salinity was not different (P = 0.56) among the canopy height classes within the two inventory blocks. The average soil pH was 3.8, and not significantly different (P = 0.98) among strata within 0–200 cm.

3.2.1. Soil carbon

Mean SOC content within the inventory blocks ranged from 17.04% at the 0–15 cm depth to 7.05% at the 180–200 cm depth, and decreased with increasing soil depth (Fig. 3c). The depth-integrated soil C content for the HTC1 to HTC3 was 11.02, 10.09 and 11.96 %C, respectively, and differences among canopy height classes (P = 0.50) and inventory blocks (P = 0.06) were not significant. The soil C density for the 0–2 m soil depth was 639.7, 608.2 and 706.8 Mg C ha^{-1} in the HTC1, HTC2 and HTC3, respectively. The differences in the mean SOC density among the three canopy height classes was insignificant (P = 0.68).

3.3. Ecosystem carbon stock

The C density of the principal pools within the ecosystem (e.g., AGB, BGB, and soils) were summed to determine an ecosystem-level C density (EC, Mg ha^{-1}) for each canopy height class (Table 2). The differences in EC among canopy height classes were primarily attributable to total biomass C (BC = AGB + BGB); where BC in HTC3 was 46.7 and 8.3 times that in HTC1 and HTC2, respectively. However, BC accounted for a small proportion of the EC, ranging from 0.5% to 28.0% with a mean of 15.3%. Correspondingly, SOC was the main component of the EC; comprising approximately 99.1, 95.2 and 71.8% of EC in HTC1, HTC2 and HTC3, respectively.

Carbon stocks of the mangroves were calculated based spatial distribution of the canopy height classes and the corresponding EC density (Table 3). Within the inventory area the EC stock was approximately 7.0 Tg C. The HTC3 contained the largest biomass C stock (0.8 Tg C) and soil C stock (2.5 Tg C). Utilizing the C density for the three canopy height classes to calculate the mangrove ecosystem C stock within Pongara National Park yielded 40.6 Tg C. As in the inventoried blocks, HTC3 had

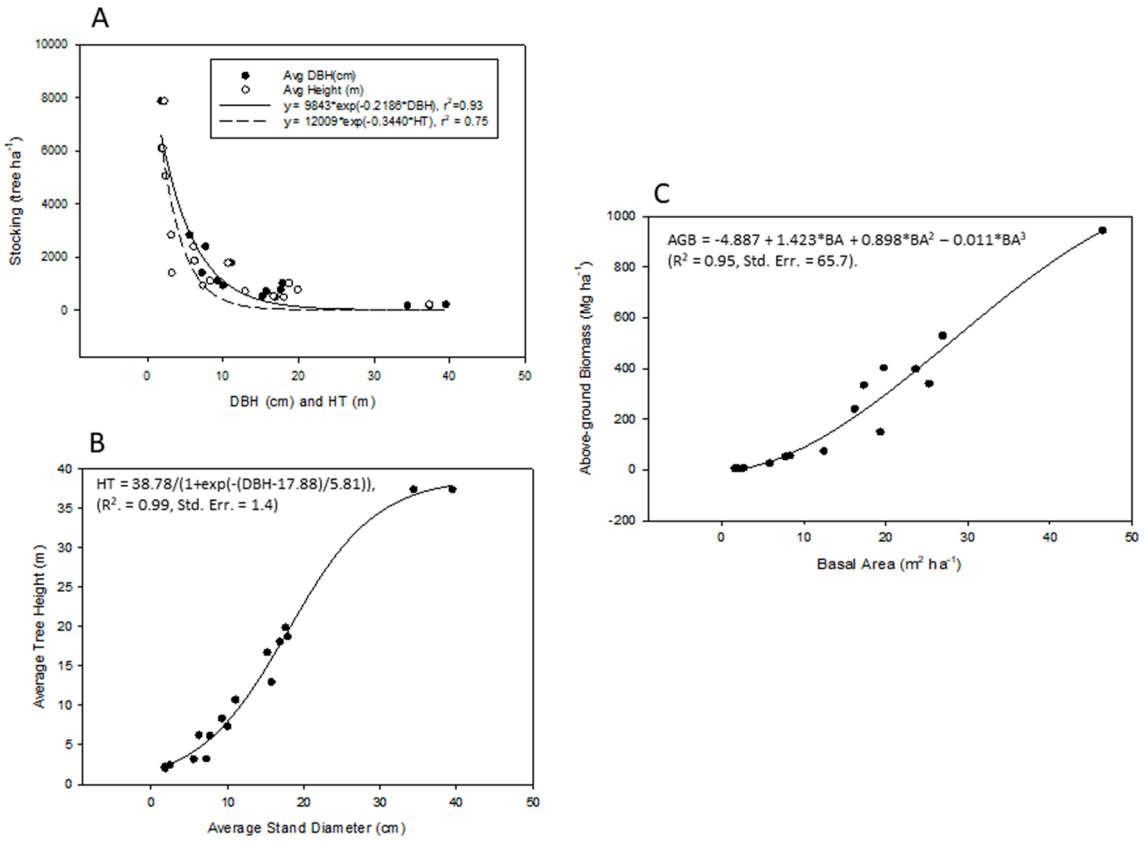

Fig. 2. Relationships among stand structure variables of mangroves in Pongara National Park, Gabon. (A) Stand stocking as a function of mean diameter at breast height (DBH) and mean tree height; (B) Relationship of mean tree height and mean stand diameter at breast height (DBH); (C) Relationship between stand basal area (BA) and above-ground biomass (AGB).

the largest biomass C stock (4.7 Tg C), but HTC1 contributed the largest soil C stock (14.7 Tg C) within the park. The soil was the main contributor to the EC stock accounting for 35.5 Tg C or approximately 88% of the EC in PNP.

4. Discussion

4.1. Forest composition and structure

The plant diversity within Pongara National Park is rich with 386 species occurring throughout the uplands and wetlands (Dauby et al., 2008). However, in the coastal forested wetlands along the Gabon estuary, *Rhizophora* was the only genus of mangroves in the inventoried area within Pongara National Park, with stands of monotypic *R. racemosa* or *R. harrisonii* represented, almost equally. Those two *Rhizophora* species are also reported to be prevalent in Nigeria (Emerhi, 2012) and central West Africa (Ajoinina et al. 2014b; Saenger and Bellan, 1995). Lebigre (1983) surveyed the distribution of mangroves in the Gabon Estuary and reported that the low-statured stands predominated within the west block, but the forest types included the occurrence of *Avicennia* in association with *Rhizophora*, which wasn't encountered in the current work. Accordingly, it may be that the *Avicennia* has been replaced by the monotypic *Rhizophora* stands. Stands of both species occurred in each of the canopy height class, and the two tallest stature stands (>35 m) were one of each species; while the tallest tree recorded was *R. racemosa* (52.5 m). Both species are reported to have a wide salinity tolerance (John and Lawson, 1990), but there was a distinct preference for *R. harrisonii* to occur in the west inventory block where the salinity was greater than the east block. In addition to having a wide tolerance to salinity, these two *Rhizophora* species tend to achieve their optimum development under the same environmental conditions (Breteler, 1969). Correspondingly, the tall-statured stands of both species also occurred in the east inventory block; however, their occurrence their occurrence is likely related to the environmental history of the area or other site factors (Woodroffe, 1993; Kathiresan and Bingham, 2001).

The development of mangrove stands are recognized to be sensitive to environmental factors (Ke et al., 2011; Yañez-Espinosa and Flores, 2011; Chen and Ye, 2014) which is likely reflected in the distribution of canopy height classes. The HTC1 and HTC2 encompassed approximately 62% of total mangrove area in PNP, and there was considerable difference in the distribution of canopy height classes between east and west inventory blocks. Trees <20 m tall covered approximately 27% of total area of the east section and over 95% of the west section of the park. Accordingly, it is likely that abiotic factors have affected the development of the mangrove stands. While high salinity levels have been reported to limit stand density, as well as height and biomass accretion in Brazilian and Nigerian mangroves (Lara and Cohen, 2006, Ukpong 1997), it's unlikely a factor in PNP, since the salinity levels are relatively low. Instead, other factors such as nutrient limitations or high sulfide concentrations (Lamers et al., 2013) may be affecting the development of the mangrove stands. Castañeda-Moya et al. (2013) reported how phosphorus, can affect productivity and biomass allocation on mixed species stands of mangroves in Florida (USA)., and that permanent flooding and high sulfide concentrations reduced above ground biomass and productivity. In PNP, the open sparsely stocked stands (included in HTC1) was typically interior from an open water edge (100+ m), similar to distribution of *R. mangle* reported in Panama (Lovelock et al., 2005). Correspondingly, is likely that the wide range in above ground biomass allocation in PNP (e.g., 2–943 Mg ha^{-1}) is related soil nutrient availability and redoximorphic conditions that are regulated by the soil water and tidal regimes.

Although the proportion of the two *Rhizophora* species were different

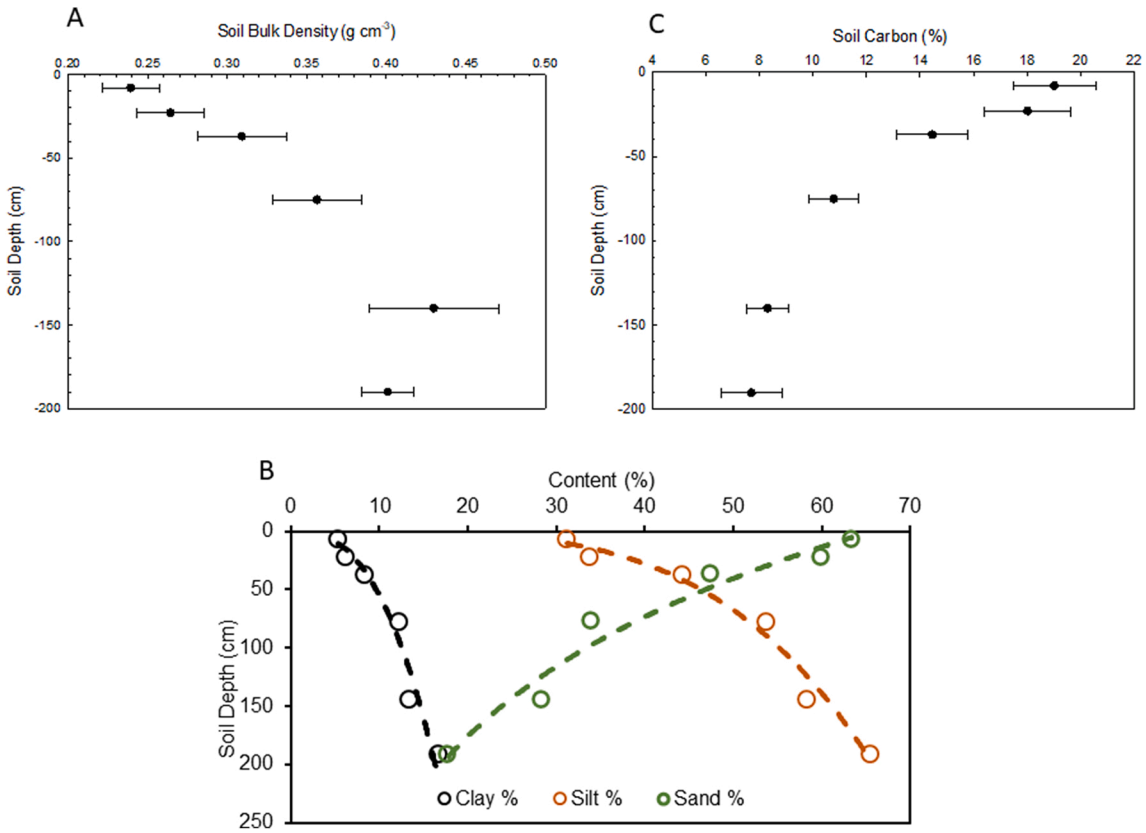

Fig. 3. Distribution of chemical and physical properties within mangrove soils in Pongara National Park, Gabon. (A) Average soil bulk density, horizonal bar = S.E., (B) Soil texture (see text for size definitions), (C) Average soil carbon. horizonal bar = S.E..

Table 2
Ecosystem carbon density (mean and standard error) and the components: above-ground (ABG) and below-ground biomass (BGB) and soil pools, for each canopy height class (HTC).

Height Class	Total AGB	Total BGB	Soil C	Ecosystem
	(Mg C ha^{-1})			
HTC1	2.5 (0.3)	2.0 (0.2)	639.7 (103.3)	644.2 (102.9)
HTC2	19.5 (7.8)	10.1 (3.7)	618.2 (61.5)	647.8 (61.3.0)
HTC3	189.2 (42.7)	53.4 (9.9)	706.8 (24.9)	949.5 (61.9)

Table 3
Ecosystem carbon stocks of mangroves in the inventoried area (east and west blocks) and the entirety of Pongara National Park. The carbon density for each of the height classes was used to estimate the C stock for the entire Park. Total biomass includes both above- and below-ground pools.

Area	Height Class	Area (ha)	Total Biomass C (Gg C)	Total Soil C (Gg C)	Total Ecosystem C (Gg C)
Inventory	HTC1	3,638	16	2,327	2,343
	HTC2	2,080	62	1,286	1,347
	HTC3	3,489	847	2,466	3,313
Total		9,207	925	6,079	7,004
Pongara	HTC1	23,023	104	14,727	14,832
National	HTC2	11,603	344	7,173	7,517
Park	HTC3	19,210	4,662	13,578	18,240
Total		53,836	5,109	35,479	40,588

among the inventoried blocks, the lack of a blocking factor effect on the structural attributes suggest that they function similarly, at least when categorized by canopy height class. The three canopy height classes were effective in classifying stands to characterize their structural attributes. The HTC1 contained the low-stature stands, while the HTC3 included a wide range of conditions from dense – tall-statured stands to "cathedral" stands. While this is the first study on mangrove structure and composition in Pongara National Park, recent work by Kauffman and Bhomia (2017) in Akanda National Park, which is approximately 50 km to the north of PNP, provides additional perspective on estuarine mangroves in Gabon. Kauffman and Bhomia (2017), measured 6 plots in what were considered "tall" mangroves (e.g. > 10 m), which corresponds approximately to HTC2 + HTC3, reported a range in tree density (750–1,400 tree ha^{-1}) that is within the reported means for HTC2 and HTC3 (2,861 and 724 trees ha^{-1}, respectively). Similarly, Ajonina et al. (2014b) reported a stocking of 1,400 trees ha^{-1}, based on 4 plots in Akanda National Park. However, stand basal area (25.4 m^2 ha^{-1}) was higher in the plots measured by Kauffman and Bhomia (2017) than the mean of 7.1–22.5 m^2 ha^{-1} measured in this inventory; but stand basal area within PNP ranged from 2.2 to 46.4 m^2 ha^{-1} (Fig. 2c). The stands in HTC3 averaged 19.9 cm DBH which is approximately double the diameter reported by Anjonina et al. (2014b); the larger diameter and lower stocking measured in PNP could account for a similar stand basal area estimate. In general, the canopy height of mangrove stands in Akanda National Park is less than PNP (Lee et al., 2018), which then suggests that stand stocking would tend to higher, and tree diameter and height lower, based on relationships with the PNP inventory data.

4.2. Biomass

Above-ground biomass was strongly related to stand basal area, which is not surprising since stand basal area effectively combines tree diameter, which is used in the allometric equation for biomass, and stocking. The value of a strong relationship between biomass and stand basal area is that it can facilitate subsequent assessments to estimate

AGB within the inventory area, using a field obtainable metric that is easier and much quicker than detailed forest plot measurements. However, the form of the biomass to stand basal area relationship (e.g., polynomial function) in this inventory is different than the linear function measured in the Zambezi River Delta, Mozambique (Trettin et al. 2015). Whether this difference in the functional relationship is due to species composition (the Zambezi River Delta has eight mangrove species in mixed stands) or other factors is unknown. Correspondingly, further work is warranted to understand the role of species composition and stand characteristics on the correlative relationship between aboveground biomass and stand basal area.

The average AGB density in West Africa is 71 Mg ha^{-1} (Tang et al., 2015), while the canopy height classes used in PNP ranged from 5 to 376 Mg ha^{-1}, encompassing the range predicted for mangroves globally (<80 to >375 Mg ha^{-1}; Hutchinson et al., 2014). The range in AGB among the inventory plots (<10 to >900 Mg ha^{-1}) exceeds the range reported by Saenger and Snedaker (1993) for 1–2° latitude, but is well within the recent global synthesis of mangrove stand data (Rovai et al., 2021). That the mangrove structural attributes within PNP span the global range attests to the value of this area for further studies on the biotic and abiotic factors affecting the structure and productivity of mangroves. The results from the inventory in PNP also demonstrate that the relationships between stand structural metrics from a specific area do not necessarily follow those derived from globally aggregated data; for example the positive relationship of stand height to AGB reported by Rovai et al. (2021) is not reflected in PNP (Suppl. Fig. 4). Reports of mangrove biomass density in Akanda National Park ranged from 341 Mg ha^{-1} (Ajonina et al. 2014) to 376 Mg ha^{-1} (Kauffman and Bhomia, 2017) are similar to the biomass density for HTC3 (376 Mg ha^{-1}) in PNP. The relative correspondence of the reported biomass density from the those studies (Ajonina et al. 2014; Kauffman and Bhomia, 2017) with that for HTC3, reflects that they do not represent the mosaic of low stature stands that comprise the majority of Akanda National Park (Lee et al., 2018). That contrast reflects the difference in synoptic assessments where sample sites are not located randomly. A systematic assessment of tropical upland forests and mangroves in Akanda National Park found that the mean AGB for mangroves was 72 Mg ha^{-1} (Goïta et al., 2019). The above-ground biomass density in the HTC1 stands, which include sparse, low-stature stands, is similar to other reports for *R. mangle* (6.8 Mg ha^{-1}, Lovelock et al., 2005) in Panama, but considerably lower than a report on *Avicennia*-dominated scrub stands in Brazil (66 Mg ha^{-1}, Virgulino-Júnior et al., 2020).

4.3. Soils

Soils within the inventoried blocks in PNP ranged in texture from sandy loam to silt loam, with the silt and sand fractions dominating. Compared to the Zambezi River Delta, a large deltaic system (Stringer et al., 2016), the soil texture in PNP (41% sand) is generally coarser than the Zambezi (<20% sand), although silt is the dominant fraction in both the deltaic system (>70%) and estuarine system of PNP (47%). In contrast to the deltaic system where the mangrove sediments were relatively uniform with depth (Stringer et al., 2016), the soils in PNP became finer with depth. Ukpong (1997) reported a loam soil in a riverine coastal setting in Nigeria that contained 20% clay, which is considerably more than the silt-dominated sediments in the Mozambique delta (Stringer et al., 2016) and Gabon estuary reported here.

Soil BD is a critical factor for estimating soil C stocks because it is used to calculate the soil C density, and small changes in bulk density propagate large changes in estimated C density. Sanderman et al. (2018) compiled a global data base for their assessment of soil C stocks in mangroves; the mean and median soil BD is 0.68 and 0.62 g cm^{-3}, respectively, which is based on over 4800 measurements (Sanderman, 2017). Accordingly, soil BD in PNP was lower than that global mean, ranging from 0.21 to 0.63 g cm^{-3} with a mean of 0.33 g cm^{-3} to 200 cm depth. Comparing the BD with soils measured in Akanda National Park, Kauffman and Bhomia (2017) report 0.35 g cm^{-3} for the 0–100 cm depth which is very close to the BD measured here (0.32 g cm^{-3}). The mean BD for PNP is also similar to reports by Donato et al. (2011) and Barreto et al. (2016). However the PNP soils were less dense than those in the Zambezi River Delta (BD = 0.84 g cm^{-3}; Stringer et al., 2016) and mangrove soils in northwestern Madagascar (BD = 0.52–1.39 g cm^{-3}; Jones et al., 2014). The BD in PNP was also lower than soils of young mangrove forests (Lunstrum and Chen, 2014) and mangrove soils along Egyptian Red Sea Coast (Eid and Shaltout, 2016).

The global median concentration of soil C in mangrove soils is 4.53% based on over 6,800 measurements (Sanderman, 2017), which is lower than the soil C concentration measured in PNP, which averaged 11.2% C. However, the SOC concentration in PNP is well within the wide range reported for mangroves globally (Barreto et al., 2016; Duarte, 2005; Kristensen et al., 2008; Adame et al., 2013; Kauffman et al., 2011). The highest mean SOC concentration was in the surface layer (17%, 0–15 cm) of the PNP soils, and it declined gradually to a mean of 7.7% C in the 180–200 cm layer. In contrast, the surface soil in a riverine mangrove stand in Nigeria were lower (6.6 %C) than the C content in mangroves within PNP (Upkong, 1997).

The soil C pool to a depth of 2 m in PNP was 639.7 ± 89.3, 618.2 ± 53.3 and 706.8 ± 23.5 Mg C ha^{-1} in HTC1, HTC2 and HTC3, respectively, with an overall mean of 654.9 ± 249.9 Mg C ha^{-1}. Using the depth integrated C density for the 0–100 cm soil depth to allow comparison with the sampled soil volumes in Akanda National Park; Kauffman and Bhomia (2017) reported 345 Mg ha^{-1} compared to 369 Mg ha^{-1} for this inventory in PNP. In sharp contrast, Ajonina et al. (2014b) report approximately 960 Mg ha^{-1}. Given the correspondence between the estimates from this inventory and Kauffman and Bhomia (2017), the reported value by Ajonina et al. (2014b) is too high; one potential factor affecting the discrepancy maybe that C concentration was estimated based on organic matter content. The C density for the total soil volume (866 Mg C ha^{-1}) reported by Kauffman and Bhomia (2017) is greater than the density measured in PNP (604 Mg C ha^{-1}); this is because they report the soil pool to a depth of 300 cm, although only one sample at most was collected below 100 cm, therefore they assume a constant concentration and soil bulk density with depth, which is not consistent with the measurements in PNP. When comparing soil C density among studies care must be taken to ensure that the sampled soil volumes are equivalent, otherwise the comparison should be done from a normalized basis.

The global median value for SOC in mangrove sediments to a depth of 1 m was recently reported as 237 Mg ha^{-1} (Ouyang and Lee, 2020). However, SOC in mangroves is recognized to vary among the various coastal geomorphic positions (Twilley et al., 2018). Rovai et al., (2018) reported a SOC content of within estuarine mangroves of approximately 30 mg C cm^{-3}, which was in the lower half among the six geomorphic positions evaluated. By comparison, the mean SOC content of soils in mangroves within PNP was 37 mg C cm^{-3}, which is well within the range reported by Rovai et al. (2018) for other estuarine systems. It's also important to note that the soil C pool in PNP was invariant with respect to stand biomass. The C density in PNP was greater than that reported in mangroves on the Zambezi River Delta of Mozambique, using the same sampling approach and depth (274–314 Mg C ha^{-1}; Stringer et al., 2016) because of the higher soil C density in the PNP estuarine mangrove system as compared the deltaic setting of the Zambezi River. In their global synthesis, Rovai et al. (2018) also found that SOC content in estuarine mangroves was greater than deltaic mangroves. However, the relationship of soil C density and biomass in mangroves from the two field-based inventories in East and West Africa is not consistent with the predicted relationship reported by Sanderman et al. (2018), which showed a positive relationship. The contrast in generalized findings between field and modeling approaches highlights the value of relatively large scale field assessments which can provide new data for subsequent model calibration and validation exercises.

Gabon is one of the few countries with a recently completed national-scale assessment of soil C stocks (Wade et al., 2019). However, due to the small area of mangroves relative to the total forest area only one inventory plot was located within mangroves, thereby precluding an estimate of soil C stocks in mangroves nationally. Comparing the upland soil C stock in Gabon with the mangroves in PNP provides a useful contrast to demonstrate the large difference between uplands and wetlands, and the need for specific wetland inventories. The national average soil C density to a depth of 2 m in Gabon is 163 Mg C ha^{-1} (Wade et al., 2019) which is 4 times less than the soil C density in mangroves of PNP (655 Mg C ha^{-1}). Accordingly, if a country developed and maintained a mangrove carbon stock inventory to supplement the C stock reported from the national forest inventory, significantly more C could be reported. Using Gabon as an example, assuming the average soil C density measured in PNP were applicable to the country which has 1,081 km^2 of mangroves (Hamilton and Casey, 2016), an additional 70.8 Tg C could be added to the national inventory.

4.4. Ecosystem carbon stocks

Ecosystem C density in the inventory blocks ranged from 644 (±89.5) to 943 (±90.9) Mg C ha^{-1}, in HTC1 and HTC3, respectively. This EC is within the range 287–1131 Mg C ha^{-1} reported by Adame et al., 2013. However, mean EC (739 Mg C ha^{-1}) was slightly lower than the values reported by Donato et al. (2011, 2012) and Kauffman et al. (2011). Again, these general comparisons are difficult without ensuring a common basis. Within Akanda National Park, Kauffman and Bhomia (2017) reported a BC of 180 Mg C ha^{-1}, which is lower than the 236 Mg C ha^{-1} reported here for the HTC3 stands. These reports affirm that the mangrove biomass C density in tall-stature stands in Gabon are greater than values reported (43–136 Mg ha^{-1}) for stands in other Central West Africa countries (Kauffman and Bhomia, 2017). However, the low-stature stands in Gabon (e.g., HTC1, HTC2) have considerable lower BC. EC often includes coarse woody debris as one of the ecosystem pools. While we have not reported this pool, Kauffman and Bhomia (2017) reported 17.1 Mg C ha^{-1}, which is effectively 3.1% of the EC, when the soil pool is normalized to 1 m depth. Accordingly, our estimates of EC will be low by that proportion, or less if a 200 cm soil depth is used.

Despite the relatively large biomass C stock in Gabon, BC is a small fraction of EC in PNP. The soil is the main contributor to the EC, accounting for 71.8% of EC in HTC3 to 99.1% in HTC1 with a mean of 84.5% of EC, which is within the range from 62% to 99% of EC reported by Donato et al. (2012), and Jones et al. (2014).

4.5. Application of remote sensing data to inventory mangroves

Forest inventories are conducted to provide objective information about the forest resources within a specified assessment area. Accordingly, plots providing the information should be distributed within the inventory area in an unbiased manner (EPA 2002). Most studies considering mangrove C stocks have been designed to address specific objectives with judgement used to locate plots; in these cases it is inappropriate to extrapolate those findings beyond their original intent. For example, the in the regional study on mangrove C stocks, Kauffman and Bhomia (2017) focused on sampling tall-statured stands within Akanda National Park in Gabon; while the report provides valuable information about those specific stands, it does not provide information about the composition of the mangrove forest landscape and the associated spatial heterogeneity. Hence those findings should not be applied generally to mangroves in Akanda National Park. Accordingly, an objective forest inventory is necessary to quantify the biomass or C stocks within a specified area for use in forest management and conservation or payment for ecosystem service (e.g., REDD+). Given the remote location of mangroves and the paucity of information about the mangroves in most countries, conducting an unbiased assessment of the mangroves is challenging.

Canopy height data derived from remote sensing data provides a very useful basis characterizing the mangrove resource prior to initiating a forest inventory because it provides information about the forest structure in a spatially explicit form. Data on the range in canopy height and the spatial distribution of stands provides a basis for stratifying the inventory area, which increases the efficiency of the inventory design (EPA 2002). That basis was used in designing the inventory of the Zambezi river delta using canopy height derived from SRTM data (Stringer et al., 2015). For this application, we used TanDEMX data (Lee et al., 2018), a high resolution data product (12 × 12 m) that enabled us to recognize two blocks with different proportions of the height classes, and to stratify the sampling using common classes. The high resolution of the TanDEM-X data also provided the capability to assess relative fine-scale nuances of the forest structure relative to geomorphic position (e.g., river, creeks and interior). To accommodate the many logistical constraints associated with working in mangroves and to objectively allocate inventory plots, a spatial decision support system (Densham, 1991; Tang et al., 2016) is a useful and necessary tool.

The application of remote sensing data to develop a canopy height model and subsequently using it to estimate above-ground biomass based on an allometric relationship is a rapidly advancing approach to inventory mangrove tracts. Lagomasino et al. (2016) tested various canopy height models developed from airborne and space platforms, and reported that while the very high resolution stereophotogrammetry model predicted canopy height of stands > 10 m in height most accurately, each of the other data (TanDEM-X, Terra-Sar-X) models produced acceptable results. The ability to accurately estimate canopy height then provides the basis to estimate above-ground standing biomass. Simard et al. (2019) utilized this approach to map mangrove canopy height globally using SRTM and GLAS data, and then applied the canopy height model to estimate above-ground biomass of countries containing the tallest mangroves, which includes Gabon. The estimated mean above-ground biomass density for mangroves in Gabon was 244 Mg ha^{-1} (Simard et al., 2019), which is greater than the area-weighted-mean AGB density in the two inventoried blocks in PNP (75 Mg ha^{-1}). PNP comprises approximately 39% of the mangroves in Gabon, hence the comparison is not an equivalent basis, although the east inventory block of PNP included the site with the highest reported density (910.5 Mg ha^{-1}) by Simard et al. (2019) as well as the inventory plot with the reported highest density (943.5 Mg ha-1). Approximately 43% of PNP is within the HTC1, which includes the sparse, low-stature stands. Accordingly, another factor may need to be included to address the challenges estimating canopy heights below 10 m (Lagomasino et al., 2016).

Other remote sensing-based approaches are also being developed to inventory mangrove structure and biomass. Pandey et al. (2019) utilized Normalized Difference Vegetation Index (NDVI) and Enhanced Vegetation Index (EVI) effectively to estimate the above-ground biomass distribution in mangroves within the Bhitarkanika Forest Reserve in India; they were also able to map the distribution of mangrove species using hyperspectral data. Testing the application of unmanned aerial vehicle (UAV) imagery to estimate mangrove biomass within the Matang Mangrove Forest Reserve (MMFR) in Malaysia, Otero et al. (2018) found the UAV data produced accurate estimates of tree height, but estimates of biomass were less accurate in mixed stands compared to stands with a single canopy layer. The challenge in applications that depend solely on canopy height is that variations in stand density are not necessarily apparent; and that variation stand density affects the allometric relationship between height and above-ground biomass.

5. Conclusions

The distribution of mangrove stands within Pongara National Park is heterogeneous. Pre-inventory information about the range in canopy height, the spatial distribution of height classes, and information about the landscape and waterways provided by high-resolution remote

sensing data facilitated the design of the inventory to accommodate stands ranging in height from 2 to 50+ m, as well as their spatial distribution. The stratified random sampling design provided an effective framework for the inventory, accommodating a wide range in forest conditions. For example, the skewed distribution of canopy heights across PNP (east to west) suggested that there may be a biophysical factor affecting stand development, so the inventory area was divided into two blocks to ensure that both settings were effectively represented. Utilization of a spatial decision support system in conjunction with the canopy height data as critical to ensuring safe and efficient field operations and objective location of the inventory plots.

The canopy height class data derived from the TanDEM-X data foretold that there would be a wide range in mangrove biomass within the inventory blocks. The area included the tallest reported mangrove tree in the world, exceedingly dense stands and areas of small-statured, widely spaced trees. Correspondingly, the mean above-ground biomass ranged from 5 to 375 Mg ha^{-1} in HTC1 to HTC3 respectively, levels that are common in the case of HTC1, to much greater than the global norm for HTC3. This range in stand development was consistent for both *Rhizophora* species; however, species distribution appears to be affected by site conditions. Accordingly, Pongara National Park would be an excellent place to study the effects of site conditions on stand composition, structure and productivity.

The soils within the two inventory blocks were relatively uniform with respect to texture, but the salinity was higher in the west block. The soil C concentration was higher than the global median and soil bulk density was approximately 50% lower. The average soil C content was not significantly different among canopy height classes, averaging 655 Mg ha^{-1} C to a depth of 2 m. The soil C density for the estuarine setting was greater than that reported for the mangroves in the Zambezi River delta in East Africa. Analogous to reports from other mangroves, the soil was the main C pool within the mangroves of PNP, accounting for approximately 84% of ecosystem C. Although the mean soil C pool in the east block (614.1 Mg C ha^{-1}) was not significantly different from that in west block (596.7 Mg C ha^{-1}), its proportion of the EC varied, 74.4% of EC in the east block and 96.7% of EC in the west block, due to the difference in biomass between these two blocks. Accordingly, all of the mangrove stands in PNP have a EC density that exceeds that of recently inventoried terrestrial forests in Gabon.

Remote sensing data and the associated tools provide much needed capabilities to quantify mangrove above-ground biomass. Those tools will continue to improve with the availability of large-scale inventories that provide spatially explicit information on forest structure and composition; data that can be used for calibrating the allometric models for above-ground biomass that are dependent on canopy height. This work also suggests how inventories of a specific land area may be used to augment national C stock estimates for wetland ecosystems that are under-represented in a national forest inventory.

Data availability

The data from the forest inventory and soil analyses are published (Trettin et al., 2020) and available at: https://www.fs.usda.gov/rds/archive/Catalog/RDS-2020-0040. Images from the field inventory area also available from that record.

CRediT authorship contribution statement

Carl C. Trettin: Conceptualization, Methodology, Investigation, Writing – Review and Re-write. **Zhaohua Dai:** Formal analysis, Writing – original draft. **Wenwu Tang:** Methodology, Software, Formal analysis. **David Lagomasino:** Investigation, Supervision. **Nathan Thomas:** Investigation. **Seung Kuk Lee:** Methodology, Software. **Marc Simard:** Conceptualization, Investigation, Supervision. **Médard Obiang Ebanega:** Investigation, Supervision. **Atticus Stoval:** Investigation. **Temilola E. Fatoyinbo:** Conceptualization, Project administrationProject administration.

Declaration of competing interest

The authors declare that they have no known competing financial interests or personal relationships that could have appeared to influence the work reported in this paper.

Acknowledgements

We would like to acknowledge the Gabon Agence Nationale des Parcs Nationaux (ANPN) for permission to work in Pongara National Park and for facilitating the field mission. CENAREST (National Center for Scientific and Technological Research) provided the research permit (No. 02740). The U.S. National Aeronautics and Space Agency (NASA) provided funding through the Carbon Monitoring Systems program for this work (#80HQTR18T0012). The inventory was coordinated with John Poulsen's Tropical Ecology Laboratory, Duke Univ. The field mission could not have been accomplished without the expert boatmen and guides from ANPN, and the energetic field assistance from students from Omar Bongo University, Libreville and Chris Beirne, Duke Univ. Comments on this manuscript by André Rovai and an anonymous reviewer were constructive and appreciated.

Appendix A. Supplementary data

Supplementary data to this article can be found online at https://doi.org/10.1016/j.ecss.2021.107432.

References

Adame, M.F., Kauffman, J.B., Medina, I., Gamboa, J.N., Torres, O., Caamal, J.P., Reza, M., Herrera-Silveira, J.A., 2013. Carbon stocks of tropical coastal wetlands within the karstic landscape of the Mexico Caribbean. PloS One 8. https://doi.org/10.1371/journal.pone.0056569.

Ajonina, G.N., 2008. Inventory and modelling mangrove forest stand dynamics following different levels of wood exploitation pressures in the Douala-Edea Atlantic coast of Cameroon, Central Africa. Mitteilungen der AbteilungenfürForstlicheBiometrie. Albert-Ludwigs- Universität Freiburg, p. 215.

Ajonina, G.N., Kairo, J., Grimsditch, G., Sembres, T., Chuyong, G., Mibog, D.E., Nyambane, A., FitzGerald, C., 2014a. Carbon Pools and Multiple Benefits of Mangroves in Central Africa: Assessment for REDD+. UNEP, Gigiri, Kenya, p. 72 (pg.).

Ajonina, G.N., Kairo, J., Grimsditch, G., Sembres, T., Chuyong, G., Diyouke, E., 2014b. Assessment of mangrove carbon stocks in Cameroon, Gabon, the Republic of Congo (RoC) and the Democratic Republic of Congo (DRC) including their potential for reducing emissions from deforestation and forest degradation (REDD+). Pg. 177-189. In: Diop, S., Barusseau, J.P., Descamps, C. (Eds.), The Land/ocean Interactions in the Coastal Zone of West and Central Africa, Estuaries of the World. Springer International Publishing, Switzerland. https://doi.org/10.1007/978-3-319-06388-1_15.

Alongi, D.M., 2011. Carbon payments for mangrove conservation: ecosystem constraints and uncertainties of sequestration potential. Environ. Sci. Pol. 14, 462–470. https://doi.org/10.1016/j.envsci.2011.02.004.

Alongi, D.M., 2012. Carbon sequestration in mangrove forests. Carbon Mgt 3, 313–322.

Attwood, T.B., Connolly, R.M., Almahasheer, H., Carnell, P.E., Duarte, C.M., Ewers-Lewis, C.J., Irigoien, X./, Kelleway, J.R.J., Lavery, P.S., Macreadie, P.I., Serrano, O., Sanders, C.J., Santos, I., Steven, A.D.L., Lovelock, C.E., 2017. Global patterns in mangrove soil carbon stocks and losses. Nat. Clim. Change 7, 523–528. https://doi.org/10.1038/NCLIMATE3326.

Baird, R., Bridgewater, L., 2017. Standard Methods for the Examination of Water and Wastewater, 23rd edition. American Public Health Association, Washington, D.C.

Barreto, M.B., Monaco, S.L., Diaz, R., Barreto-Pittol, E., Lopez, L., Peralla, M.d.C.R., 2016. Soil organic carbon of mangrove forests (*Rhizophora* and *Avicennia*) of the Venezuelan Caribbean coast. Org. Geochem. 100, 51–61.

Breteler, F.J., 1969. The Atlantic species of *Rhizophora*. Acta Bot. Neerl. 18, 434–441.

Carsan, S., Orwa, C., Harwood, C., Kindt, R., Stroebel, A., Neufeldt, H., Jamnadass, R., 2012. African Wood Density Database. World Agroforestry Centre, Nairobi. http://apps.worldagroforestry.org/treesnmarkets/wood/index.php#.

Castañeda-Moya, E., Twilley, R.R., Rivera-Monroy, V.H., 2013. Allocation of biomass and net primary productivity of mangrove forests along environmental gradients in the Florida Coastal Everglades. USA. For. Ecol. Mgt. 367, 226–241. https://doi.org/10.1016/j.foreco.2013.07.011.

Chen, Y., Ye, Y., 2014. Effects of salinity and nutrient addition on mangrove *Excoecaria agallocha*. PLOS 9, 1–11.

Dauby, G., Leal, M., Stévart, T., 2008. Vascular plant checklist of the National Park of Pongara. Gabon. Syst. Geogr. Plants 78, 155–216.

Densham, P.J., 1991. Spatial decision support system. In: Maguire, D.J., Goodchild, M.F., Rhind, D. (Eds.), Geographical Information System: Principles and Applications, vol. 1. principles, John Wiley and Sons, New York, pp. 403–412.
Donato, D.C., Kauffman, J.B., Murdiyarso, D., Kurnianto, S., Stidham, M., Kanninen, M., 2011. Mangroves among the most carbon-rich forests in the tropics. Nat. Geosci. 4, 293–297.
Donato, D.C., Kauffman, J.B., Mackenzie, R.A., Ainsworth, A., Pfleeger, A.Z., 2012. Whole-island carbon stocks in the tropical Pacifi: implications for mangrove conservation and upland restoration. J. Environ. Manag. 97, 89–96.
Duarte, C.M., Middelburg, J.J., Caraco N., 2005. Major role of marine vegetation in oceanic carbon cycle. Biogecosciences 2, 1–8. https://doi.org/10.5194/bg-2-1-2005.
Eid, E.M., Shaltout, K.H., 2016. Distribution of soil organic carbon in the mangrove *Avicennia marina* (Forssk.) Vierh. Along the Egyptian Red Sea coast. Regional Studies in Marine Science 3, 76–82.
Emerhi, E.A., 2012. Variations in anatomical properties of *Rhizophora racemosa* (Leechm) and *Rhizophora Harrisonii* (G.mey) in a Nigerian mangrove forest ecosystem. Int. J. For. Soil Eros. (IJFSE) 2, 89–96.
Environmental Protection Agency (EPA), 2002. Guidance on Choosing a Sampling Design for Environmental Data Collection. US Environmental Protection Agency, Washington, D.C, p. 178 pg. EPA/240/R-02/005.
FAO, 2007. The World's Mangroves 1980-2005. Food and Agriculture Organization of the United Nations, Rome, Italy.
Fatoyinbo, T.E., Simard, M., 2013. Height and biomass of mangroves in Africa from ICESat/Glas and SRTM. Int. J. Rem. Sens. 34, 668–681. https://doi.org/10.1080/01431161.2012.712224.
Feliciano, E., Wdowinski, S., Potts, M.D., Lee, S.K., Fatoyinbo, T.E., 2017. Estimating mangrove canopy height and above-ground biomass in the everglades National Park with lidar and TanDEM-X data. Rem. Sens. 9, 702. https://doi.org/10.3390/rs9070702.
Friess, D.A., Webb, E.L., 2014. Variability in mangrove change estimates and implications for the assessment of ecosystem service provision. Global Ecol. Biogeogr. 23, 715–725. https://doi.org/10.1111/geb.12140.
Friess, D.A., Krauss, K.W., Taillardat, P., Adame, M.F., Yando, E.S., Cameron6, C., Sasmito, S.D., Sillanpää, M., 2020. Mangrove blue carbon in the face of deforestation, climate change and restoration. Ann. Plant Rev. 3, 427–456.
Giri, C., Ochieng, E., Tieszen, L.L., Zhu, Z., Singh, A., Loveland, T., Masek, J., Duke, N., 2011. Status and distribution of mangrove forest of the world using earth observation satellite data. Global Ecol. Biogeogr. 20, 154–159.
Goïta, K., Mouloungou, J., Bénié, G.B., 2019. Estimation of aboveground biomass and carbon in a tropical rain forest in Gabon using remote sensing and GPS data. Geocarto Int. 34, 243–259.
Goldberg, L., Lagomasino, D., Thomas, N., Fatoyinbo, T., 2020. Global declines in human driven mangrove loss. 2020. Global Change Biol. 25, 5844–5855. https://doi.org/10.1111/gcb.15275.
Hamilton, S.E., Casey, D., 2016. Creation of a high spatio-temporal resolution global database of continuous mangrove forest cover for the 21st century (CGMFC-21). Global Ecol. Biogeogr. 25, 729–738.
Hamilton, S.E., Friess, D.A., 2018. Global carbon stocks and potential emissions due to mangrove deforestation from 2000 to 2012. Nat. Clim. Change 8, 240–244. https://doi.org/10.1038/s41558-018-0090-4.
Himans, R.J., Cameron, S.E., Parra, J.L., Jones, P.G., Jarvis, A., 2005. Very high resolution interpolated climate surfaces for global land areas. Int. J. Climatol. 25, 1965–1978.
Hutchinson, J., Manica, A., Swetnam, R., Balmford, A., Spalding, M., 2014. Predicting global patterns in mangrove forest biomass. Conservation Letters 7, 233–240. https://doi.org/10.1111/conl.12060.
IPCC, 2019. Special Report on the Ocean and the Cryosphere. https://www.ipcc.ch/srocc/.
John, D.M., Lawson, G.W., 1990. A review of mangrove and coastal ecosystems in West Africa and their possible relationships. Estuar. Coast Shelf Sci. 31, 505–518.
Jones, T.G., Rastsimba, H.R., Ravaoarinorotsohoarana, L., Cripps, G., Bey, A., 2014. Ecological variability and carbon stock estimates of mangrove ecosystem in Northwestern Madagascar. Forests 5, 177–205.
Kathiresan, K., Bingham, B.L., 2001. Biology of mangroves and mangrove ecosystems. Adv. Mar. Biol. 40, 81–251.
Kauffman, J.B., Heider, C., Cole, T.G., Dwire, K.A., Donato, D.C., 2011. Ecosystem carbon stocks of Micronesian mangrove forests. Wetlands 31, 343–352.
Kauffman, J.B., Donato, D.C., 2012. Protocols for the Measurement, Monitoring and Reporting of Structure, Biomass and Carbon Stocks in Mangrove Forests. Working Paper 86. CIFOR, Bogor, Indonesia.
Kauffman, J.B., Bhomia, R.K., 2017. Ecosystem carbon stocks of mangroves across broad environmental gradients in West-Central Africa: global and regional comparisons. PloS One 12 (11), e0187749. https://doi.org/10.1371/.journal.pone.0187749.
Ke, L., Zhang, C., Guo, C., Lin, G.H., Tam, N.F.Y., 2011. Effects of environmental stresses on the responses of mangroves plants to spent lubricating oil. Mar. Pollut. Bull. 63, 385–395.
Kristensen, E., Bouillon, S., Dittmar, T., Marchand, C., 2008. Organic carbon dynamics in mangrove ecosystems: a review. Aquat. Bot. 89, 201–219.
Lagomasino, D., Fatoyinbo, T., Lee, S.K., Feliciano, E., Trettin, C., Simard, M., 2016. Comparison of mangrove canopy height using multiple independent measurements from land, air, and space. Rem. Sens. 8, 327. https://doi.org/10.3390/rs8040327.
Lamers, L.P.M., Govers, L.L., Janssen, I.C.J.M., Geurts, J.J.M., Vander Welle, M.E.W., Van Katwijk, M.M., Vander Heide, T., Roelofs, J.G.M., Smolders, A.J.P., 2013. Sulfides as a soil phytotoxin: a review. Front. Plant Sci. 4, 268. https://doi.org/10.3389/fpls.2013.00268.
Lara, R.J., Cohen, M.C.L., 2006. Sediment porewater salinity, inundation frequency and mangrove vegetation height in Bragança, North Brazil: an ecohydrology-based empirical model. Wetland Ecol. Mgt. 14, 349–358.
Lebigre, J.-M., 1983. Les mangroves des rias du littoral gabonais. Essai de cartographie typologique. Rev. Bois et Forêts des Tropiques 199, 3–28.
Lee, S.K., Fatoyinbo, T.E., Lagomasino, D., Feliciano, E., Trettin, C., 2018. Multibaseline TanDEM-X mangrove height estimation: the selection of the vertical wavenumber. IEEE J Selected Topics in Applied Earth Observation and Remote Sensing. https://doi.org/10.1109/JSTARS.2018.2835647.
Locatelli, T., Binet, T., Kairo, J.G., King, L., Madden, S., Patenaude, G., Upton, C., Huxham, M., 2014. Turning the tide: how blue carbon and payments for ecosystem services (PES) might help save mangrove forests. Ambio 43, 981–995.
Lovelock, C.E., Feller, I.C., McKee, K.L., Thomipson, R., 2005. Variation in mangrove forest structure and sediment characterics in Bocas del Toro, Panama. Caribb. J. Sci. 41, 456–464.
Lunstrum, A., Chen, L., 2014. Soil carbon stocks and accumulation in young mangrove forests. Soil Biol. Biochem. 75, 223–232.
Ong, J., 1995. The ecology of mangrove conservation and management. Hydrobiologia 295, 343–351.
Otero, V., De Kerchove, R.V., Satyanarayana, B., Martínez-Espinosa, C., Fisol, A.M.B., Ibrahim, M.R.B., Mohd-Lokman, I.S.H., Lucas, R., Dahdouh-Guebas, F., 2018. Managing mangrove forests from the sky: forest inventory using field data and Unmanned Aerial Vehicle (UAV) imagery in the Matang Mangrove Forest Reserve, peninsular Malaysia. For. Ecol. Mgt. 411, 35–45. https://doi.org/10.1016/j.foreco.2017.12.049.
Ouyang, X., Lee, S.Y., 2020. Improved estimates of global carbon stock and carbon pools in tidal wetlands. Nat. Commun. 11, 317. https://doi.org/10.1038/s41467-019-14120-2.
Pandey, P.C., Anand, A., Srivastava, P.K., 2019. Spatial distribution of mangrove forest species and biomass assessment using field inventory and earth observation hyperspectral data. Biodivers. Conserv. 28, 2143–2162. https://doi.org/10.1007/s10531-019-01698-8.
Ramsar Sites Information Sheet, 2015. Parc National Pongara. Ramasar Site No. 1653. https://rsis.ramsar.org/ris/1653.
Rovai, A.S., Twilley, R.R., Castañeda-Moya, E., Riul, P., Cifuentes-Jara, M., Manrow-Villalobos, M., Horta, P.A., Simonassi, J.C., Fonseca, A.L., Pagliosa, P.R., 2018. Global controls on mangrove carbon storage in soils. Nature Climate Chg 534 (8), 534–538. https://doi.org/10.1038/s41558-018-0162-5.
Rovai, A., Twilley, R.R., Castañeda-Moya, E., Midway, S.R., Friess, D.A., Trettin, C.C., Bukoski, J.J., Stovall, A.E.L., Pagliosa, P.R., Fonseca, A.L., Mackenzie, R.A., Aslan, A., Sasmito, S.D., Sillanpää, M., Cole, T.G., Purbopuspito, J., Warren, M.W., Murdiyarso, D., Mofu, W., Sharma, S., Tinh, P.H., Riul, P., 2021. Macroecological patterns of forest structure and allometric scaling in mangrove forests. Global Ecol. Biogeogr. 30, 1000–1013. https://doi.org/10.1111/geb.13268.
Saenger, P., Snedaker, S.M., 1993. Pantropical trends in mangrove biomass and annual litterfal. Oecologia 96, 293–299.
Saenger, P., Bellan, M.F., 1995. The Mangrove Vegetation of Atlantic Coast of Africa: a Review. Université de Toulouse, Toulouse, France. Southern Cross University ePublication@SCU.
Sanderman, J., 2017. Global Mangrove Soil Carbon: Dataset and Spatial Maps, Harvard Dataverse, V4, UNF:6:KdgZjEsAGV1VOL82caK6JQ==[fileUNF]. https://doi.org/10.7910/DVN/OCYUIT.
Sanderman, J., Hengl, T., Fiske, G., Solvik, K., Adame, M.F., Benson, L., 18 others, 2018. A global map of mangrove forest soil carbon at 30m spatial resolution. Environ. Res. Lett. 13, 055002 https://doi.org/10.1088/1748-9326/aabe1c.
Simard, M.K., Zhang, V.H., Rivera-Monroy, Ross, M.S., Ruiz, P.L., Castañeda-Moya, E., Twilley, R.R., Rodriguez, E., 2006. Mapping height and biomass of mangrove forests in Everglades National Park with SRTM elevation data. Photogramm. Eng. Rem. Sens. 72, 299–311.
Simard, M.L., Fatoyinbo, L., Smetanka, C., Rivera-Monroy, V.H., Castañeda-Moya, E., Thomas, N., Van der Stocken, T., 2019. Mangrove canopy height globally related to precipitation, temperature and cyclone frequency. Nat. Geosci. 12, 40–45. https://doi.org/10.1038/s41561-018-0279-1.
Shapiro, A.C., Trettin, C.C., Küchly, H., Alavinapanah, S., Bandeira, S., 2015. The mangroves of the Zambezi delta: increase in extent observed via satellite from 1994 to 2013. Rem. Sens. 7, 16504–16518. https://doi.org/10.3390/rs71215838.
Stringer, E.C., Trettin, C.C., Zarnoch, S.J., Tang, W., 2015. Carbon stocks of mangroves within the Zambezi river delta, Mozambique. For. Ecol. Mgt. 354, 139–148.
Stringer, E.C., Trettin, C.C., Zarnoch, S.J., 2016. Soil properties of mangroves in contrasting geomorphic settings within the Zambezi River Delta, Mozambique. Wetl. Ecol. Manag. https://doi.org/10.1007/s11273-015-9478-3.
Tang, W., Feng, W., Jia, M., Shi, J., Zuo, H., Trettin, C., 2015. The assessment of mangrove biomass and carbon in West Africa: a spatially explicit analytical framework. Wetl. Ecol. Manag. https://doi.org/10.1007/s11273-015-9474-7.
Tang, W., Feng, W., Jia, M., Shi, J., Zuo, H., Stringer, C.E., Trettin, C.C., 2016. A cyber-enabled spatial decision support system to inventory mangroves in Mozambique: coupling scientific workflows and cloud computing. Int. J. Geogr. Inf. Sci. https://doi.org/10.1080/13658816.2016.1245419.
Thomas, G.W., 1996. Soil pH and soil acidity. In: Methods of Soil Analysis: Part 3-Chemical Methods. Soil Science Society of America, Madison, Wisconsin, pp. 475–490.
Thomas, N., Lucas, R., Bunting, P., Hardy, A., Rosenqvist, A., Simard, M., 2017. Distribution and drivers of global mangrove forest change, 1996 – 2010. PloS One 12 (6), e0179302. https://doi.org/10.1371/journal.pone.0179302.
Trettin, C.C., Stringer, C.E., Zarnoch, S.J., 2015. Composition, biomass and structure of mangroves within the Zambezi river delta. Wetl. Ecol. Manag. 24, 173–186.

Trettin, Carl C., Dai, Zhaohua, Tang, Wenwu, Lagomasino, David, Thomas, Nathan, Lee, Seung-Kuk, Ebanega, Médard Obiang, Simard, Marc, Fatoyinbo, Temilola E., 2020. Carbon Stock Inventory of Mangroves. Pongara National Park, Gabon. Fort Collins, CO. https://doi.org/10.2737/RDS-2020-0040. Forest Service Research Data Archive.

Twilley, R.R., Rovai, A.S., Riul, P., 2018. Coastal morphology explains coastal blue carbon distributions. Front. Ecol. Environ. 16 (9), 503–508. https://doi.org/10.1002/fee.1937.

Upkong, I.E. Vegetation and its relationship to soil nutrients and salinity in the Calabar mangrove swamp, Nigeria. Mangroves Salt Marshes 1:211-281.

Van der Werf, G.R., Morton, D.C., DeFries, R.S., Olivier, J.G.J., Kasibhatla, P.S., Jackson, R.B., Collatz, G.J., Randerson, J.T., 2009. CO_2 emissions from forest loss. Nat. Geosci. 2, 737–738.

Virgulino-Júnior, P.C.C., Carneiro, D.N., Nascimento Jr., W.R., Cougo, M.F., Fernandes, M.E.B., 2020. Biomass and carbon estimation for scrub mangrove forests and examination of their allometric associated uncertainties. PloS One 15 (3), e0230008. https://doi.org/10.1371/journal. pone.0230008.

Wade, A.M., Richter, D.D., Medjibe, V.P., Bacon, A.R., Heine, P.R., White, L.J.T., Poulsen, J.R., 2019. Estimates and determinants of stocks of deep soil carbon in Gabon, Central Africa. Geoderma 341, 236–248.

Woodroffe, C.D., 1993. Geomorphological and climatic settings and the development of mangrove forests. Pg. 13-20. In: Lieth, H., Al Masoom, A.A. (Eds.), Towards the Rational Use of High Salinity Tolerant Plants -, vol. 1. Springer Science +Business Media, Dordrecht.

Yañez-Espinosa, L., Flores, J., 2011. A review of sea-level rise effect on mangrove forest species: anatomical and morphological modifications. Pg. 253-276. In: Casalegno, S. (Ed.), Global Warming Impacts – Case Studies on the Economy, Human Health, and on Urban and Natural Environments. InTech, Croatia.